IEEE Access
Multidisciplinary | Rapid Review | Open Access Journal

Received December 1, 2019, accepted January 7, 2020, date of publication January 10, 2020, date of current version January 17, 2020.

Digital Object Identifier 10.1109/ACCESS.2020.2965616

The Novel Mobility Models Based on Spiral Line for Aerial Backbone Networks

DAWEI HE, WEI SUN, AND LEI SHI
Space Science Department, University of Xidian, Xi'an CO 710126, China
Corresponding author: Dawei He (252642902@qq.com)

This work was supported in part by the National Nature Science Foundation of China (NSFC) under Grant 61671356.

ABSTRACT With the convenience and flexibility, the UAV has received more attention in the search and rescue. Due to inherent mobility of UAV, the aerial backbone network maybe suffers some problems of dynamics of connectivity, such as uncertain delay jitter or occasional connection interruption. However, the existing mobility model could not accurately capture aerial mobility without the smooth trajectory and the capacity of rapid coverage. In this paper, we propose a novel mobility model based on spiral line (SLMM) for aerial backbone network. Firstly, we describe the background and related work. Then, we propose the basic concept and advantages of SLMM. In addition, we investigate the mathematical feature of SLMM. Besides, we propose some novel mobility metrics and analyze quantitatively the mobility feature of SLMM through simulation. Finally, we evaluate the network performance under the SLMM. The result show that the SLMM has the smooth trajectory and the uniform distribution of spatial nodes at steady state. In addition, covering the zone of area of 16pi the aerial node merely take almost 27s under the SLMM. Meanwhile, the convergence time could be adjusted by changing the internal parameters. Moreover, the aerial backbone network could approach the throughput of 0.43Mb/s, the end-to-end delay of 4.42ms and the packet loss rate of nearly 0.00%。 under the SLMM, and the best choice of routing strategy is the AODV protocol. We believe that the SLMM as a significant supplement of mobility model can provide the helpful guideline in the design and analysis of aerial backbone network.

INDEX TERMS Aerial backbone network, mobility model, rapid coverage, smooth trajectory.

I. INTRODUCTION

In recent years, the issue of urban security has received more attention, especially in disaster. The rescue workers and vehicles should cooperate with each other to complete rescue in case of disaster [1]. Searching and locating victims as the key step determines the success of rescue, because the searching time maybe largely affects the survival rate of survivors. As we known, the golden time is less than 72 hours for rescue, after that the survival rate will sharply decline, even the survival time is less than 20 minute for avalanche [2]. Therefore, the searching mission is foremost for rescue.

With the convenience and flexibility, the UAV is a good choice for searching mission. The UAV could rapidly search and accurately locate the victim, thereby the ground rescue could directly reach the target location. On the other hand, the unique issue of UAV, such as the security and the limitation of power, should be cautiously considered [3]. Moreover, the inherent mobility which causes the problem of dynamics of connectivity (e.g. the frequent variations of network topology and intermittent connection [4]) severely affects the network performance [5]. As a result, the previous connection between aerial nodes maybe is interrupted which will largely influence the efficiency of rescue. Hence, a reliable aerial backbone network is required [6].

Compared with other networks, the routing protocol (e.g. DSDV and AODV [7]) which are seriously influenced by high mobility determine the property of aerial network, includes network throughput, end-to-end delay and packet loss rate [8]. Therefore, an authentic mobility model is an important foundation for aerial backbone network [9]. In the existing mobility model, the random mobility model (RMM), such as RWP and RPGM [10], which capture the random movement of human or vehicle has been studied in the MANET or VANET. Unfortunately, the basic RMM is not suitable for the aerial scenario with the change of

The associate editor coordinating the review of this manuscript and approving it for publication was Mohammad S. Khan.

sharp direction. To overcome the drawback of RMM, some synthetic RMM has been proposed, such as Gauss Markov Model [8] and distributed phenomenon repel model [11]. In addition, the traces-based RMM (e.g. [12], [13]) which utilizes the actual traces also is developed.

However, they lack enough space-time correlation caused by mechanical and aerodynamic constraint, thereby could not accurately capture aerial mobility. Moreover, it is no doubt that a realistic aerial mobility model (AMM) should support different requirements in different applications. Hence, the application-driven AMM is an optimal choice [9]. Nevertheless, the existing AMM, such as SRCM [15] and ST [9], [14], could not capture the space-time correlation in aerial scene without smooth trajectory. For example, it is impossible for aerial flight that the node occurs the change of sharp direction under the SRCM model switching the adjacent trajectory. Similarly, the ST model occasionally produces some unreal switching points at the adjacent interval. Importantly, they could not rapidly search and cover the disaster area due to the existence of extra path. Therefore, a realistic and application-driven AMM should be developed.

In this paper, we propose a novel AMM based on spiral line (SLMM) for aerial backbone network. First of all, we describe background of SAR and some specific requirements of AMM. Besides, we review some related works to investigate whether the existing mobility model could satisfy these requirements of AMM. Next, we introduce the basic concept and characteristics of SLMM. Then, we systematically investigate some mathematical features of SLMM, includes the expression, the probability density function (PDF) and the frequency density function (FDF). The result shows that the SLMM has the specific expression, the PDF of uniform distribution and the FDF of highly symmetric distribution. In addition, we propose some novel metrics to quantitative analyzes mobility features of SLMM through simulation (e.g. smoothness, coverage, boundary and randomness). The result shows that these measures are valid under different mobility model and the SLMM possesses not only smooth trajectory, but also superior and flexible capacity of coverage. Finally, we evaluate the network performance under the SLMM. The simulation reveals that compared with other mobility models the aerial backbone network has the higher network throughput, lower end-to-end delay and lower packet loss rate under the SLMM.

To our best knowledge, the SLMM is first authentic AMM which possesses smooth trajectory, the capacity of superior coverage and outstanding network performance, thereby it could be directly deployed in the actual scene to help design optimal aerial backbone networks. Hence, we believe that the SLMM as a valuable extension of AMM will motivate more effort on the relevant research in the future.

The rest of this paper is organized as follows. In Section II, we describe background and related work. Then, we introduce the basic concept and characteristics of SLMM in Section III. In addition, we discuss some mathematical features of SLMM in Section IV. Besides, we define some novel metrics of mobility of AMM in Section V. In Section VI, we investigate some mobility features of SLMM through simulation. Moreover, we evaluate the network performance under the SLMM in Section VII. Finally, we give conclusion and future work in Section VIII.

II. BACKGROUND AND RELATED WORK

In this section, we will describe background and related work. Firstly, we introduce background and main features of SAR. Then, we discuss some specific requirements of AMM in the SAR. Finally, we briefly review related works about the mobility model.

A. THE BACKGROUND AND MAIN FEATURE

While the disaster happens, the rescue team should search and carry victims out of disaster area. Then, the medical worker simply dresses the wound of victims and transports them to the hospital by ambulances or helicopters [1]. Thus, the SAR mission mainly undertakes searching and locating victims [2].

Due to convenience and flexibility, the unmanned aerial vehicle (UAV) perfectly replaces the rescue team to perform the SAR mission [43]. Once finding a victim, the UAV will communicate with the ground rescue, thereby they can immediately reach the target location [44]. Hence, the UAV undertaking the SAR mission will lead role in future rescues (e.g. [16]–[18]).

Although the UAV largely helps to rescue, it should follow some constraints of SAR. The foremost one is the effectiveness of time. In other words, the UAV should search the target zone with few times, because the searching time largely affects the survival rate of survivors. Besides, the number of nodes do not exceed 20 [2]. It means that the aerial backbone network constructed by aerial nodes is the sparse network [46]. In addition, the UAV should search the target zone around the potential center. Once the uncommon case occurs the UAV could hover over current location. Thus, the UAV keeps moderate speed, commonly less than 25m/s [19]. Limited the battery capacity, the UAV could carry the communication devices with the connected range of 200m [2], [45]. Finally, it is important for SAR that the UAV uniformly searches the disaster zone to ensure each victim has the fair chance to receive rescue.

In addition, some rules should be considered. Firstly, the typical aerial feature is the smoothness of trajectory caused by the mechanical and aerodynamic constraints (i.e. the high space-time correlation) [9]. And the searched area is approximately on the order of kilometers [20]. In addition, the aerial channel is the similar space of two path, because the most obstacle, such as structures and infrastructures, has been destroyed by disaster or rescue worker [1], [47].

B. THE Specific REQUIREMENT OF AMM

As discussed above, some main features of SAR are as follows.

1) The limitation of the ending time, the quantity of nodes, the maximum speed, the connected range and the size of scenario.

2) The requirement of hovering, searching rapidly and fairly and the search center.

3) The physical rules of the smooth trajectory and the aerial environment of two path.

Thus, an authentic AMM should follow these constraints, thereby could accurately capture aerial mobility in the SAR. In addition, an optimal AMM also follows some requirements of mobility model [5].

1) Capturing accurately the mobility pattern in the specific scenario.

2) Having mathematically and statistically tractable to understand its theoretical limitation.

3) Being flexible enough to produce different mobility pattern by adjusting internal parameters.

Next, we briefly review some related works to investigate whether the existing mobility model could satisfy these requirements of AMM, especially the smoothness of trajectory and the capacity of rapid coverage.

C. THE RELATED WORK ABOUT MOBILITY MODEL

The preliminary mobility model has developed in the MANET and VANET to simulate the movement of human or vehicles [10]. For example, the random movement that some humans and pets wander within the specific zone could be captured by random walk model (RW) [21] or random waypoint model (RWP), which could be usually used to evaluate the network performance [22]. In addition, the random direction model (RD) has been utilized to model the ground movement [23]. Specially, the group mobility model in which each node has a logical center of movement, such as reference point group model (RPGM) [24], [25] and extension versions of RPGM [10], are proposed to capture the mobility of group of humans or vehicles.

These random mobility models (RMM) could capture some simple movement with the low complexity [10]. Nevertheless, they do not have the smooth trajectory due to some inherent defects of RMM, such as the change of sharp direction (see Figure 1) and the jump of speed. Importantly, with the extra path the aerial node could not rapidly search and cover the target zone under the RMM. Thus, the RMM is not suitable for the aerial scenario.

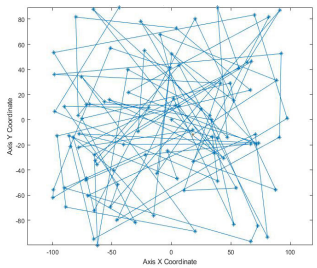

FIGURE 1. The trajectory of RWP.

To overcome inherent drawback of RMM, the modified version of RMM which has a certain degree of space-time correlation are proposed, includes the spatial and temporal dependencies mobility model (STDMM) [5], the Gaussian-Markov model (GM) [8], and the probabilistic version of RW model [10]. In addition, the Body Gaussian-Markov model (BGMM) has been proposed in recent work to simulate the random movement of wireless body area network (WBAN) [42]. Similarly, they could capture simple mobility of human or vehicle without the change of sharp direction [8], [10]. However, a certain degree of space-time correlation is not enough to ensure the smooth trajectory of aerial node. In addition, the aerial node also exists extra paths under the modified version of RMM, thereby do not have the capacity of rapid coverage. Thus, the modified version of RMM is not authentic for aerial environment.

Due to the diversity of aerial scene, the application-driven AMM is proposed which could satisfy some special requirements in the specific scene [2], [4]. For example, the distributed pheromone-repel mobility model (DPR) is presented to meet the specific requirement in the reconnaissance [11]. The DPR model introduces the concept of pheromone, and develops the probabilistic version of RMM to capture the random movement of group. Intuitively, the logic of phenomenon could enhance coordination within the group, thereby reduce extra paths. Thus, the DPR model has the chance to rapidly cover the target zone. Unfortunately, the DPR model could not satisfy the requirement of smooth trajectory without enough space-time correlation (see Figure 2). Hence, the DPR model is not credible for aerial scene.

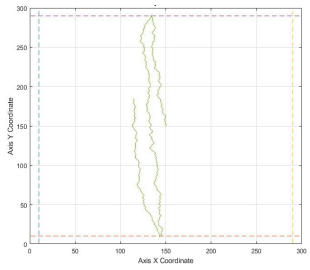

FIGURE 2. The trajectory of DPR.

Similarly, the smooth-turn model (ST) is proposed in the aerial reconnaissance [9], [14]. Compared with the DPR the ST has more space-time correlation, thereby it can ensure that aerial node could keep smooth trajectory in most cases [9]. Regretfully, the ST occasionally occur some unsmooth switching points at the adjacent intervals (see Figure 3), such that it cannot meet the requirement of smooth trajectory. Moreover, absented the potential searching center the aerial node maybe repetitively search the visited zone under the ST, thus it could not guarantee the capacity of rapid coverage. Importantly, the ST could support some 3D movement, such as Z-dependent and Z-independent [14], which is ignored in other mobility model.

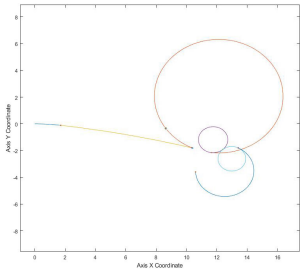

FIGURE 3. The trajectory of ST.

Aimed to aerial transportation, the flight-plan mobility model (FP) has been proposed in which the aerial node follows the waypoint defined on the map [7], [26]. In fact, the FP could be viewed as the case of RWP in essence [7], thereby also has some inherent defects of RWP. Hence, the FP also is not suitable for aerial scene, but it could roughly capture aerial mobility in the wide scene [26]. Similarly, the FP also allows 3D movement within the wide 3D space. Therefore, the FP model is credible in some scenarios (e.g. aerial transportation or cruise).

Faced with the search and rescue, the semi-random circular movement mobility model (SRCM) is proposed in which the aerial node could search the target zone around the potential center [15]. Similarly, the SRCM also possesses a certain degree of space-time correlation, thereby it could ensure that the aerial node keeps the smooth trajectory in most cases. Regretfully, switching to next circular trajectory the aerial node inevitably occurs some unsmooth points caused by the change of sharp direction under the SRCM (see Figure 4). In addition, the SRCM also exists unnecessary paths, such that it could not provide the capacity of rapid coverage. Hence, the SRCM is not authentic for aerial flight.

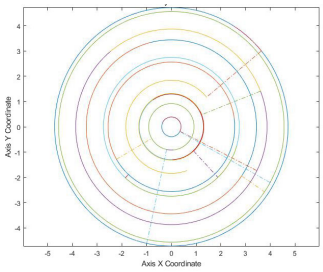

FIGURE 4. The trajectory of SRCM.

Except RMM and synthetic AMM, some traces-based mobility model became a hot issue, which introduces some mobility pattern measured in the actual traces (e.g. [1], [5], [12], [13], [15], [27]). But, it is a tough challenge that collecting a credible trace in the actual scene [5]. Certainly, the existing mobility model, such as RMM and synthetic AMM, could not accurately capture aerial mobility without the smooth trajectory. Meanwhile, they could not provide the capacity of rapid coverage due to the existence of extra paths. In addition, they also lack specific expression except the GM, which adds a certain degree of complexity of mathematical analysis. Besides, they could not produce a wide range of different mobility pattern by adjusting some internal parameters.

In short, the existing mobility model is not enough to satisfy the specific requirement of AMM in the SAR. Therefore, the realistic and application-driven AMM which has smooth trajectory and rapid coverage should be developed.

Next, we will introduce the basic concept of SLMM, such as the mechanism and the novel boundary model.

III. MOBILITY MODEL BASED ON SPIRAL LINE

In this section, we will introduce the basic concept of SLMM. Firstly, we describe the mechanism of SLMM and give the synthetic trajectory. In addition, we validate the synthetic trajectory of SLMM through real traces. Then, we elaborate the novel boundary model in the SLMM. Finally, we intuitively analyze the characteristics and advantages under the SLMM.

A. THE MECHANISM OF SLMM

In order to closely capture aerial mobility, we present some assumptions of mobility in the SLMM. Firstly, we utilize angular speed to reflect the speed of aerial node, and assumed that it is the uniform distribution within the certain range. Then, the moving time interval is the exponential distribution with the certain coefficient, and the pausing time interval is the uniform distribution within the certain range. In addition, the thread pitch of spiral line is half of connected range of devices, and the initial position of aerial node is the origin of coordinate.

With these assumptions, we then introduce the mechanism of SLMM. For the sake of clarity, we give the synthetic trajectory of SLMM at first (see Figure 5).

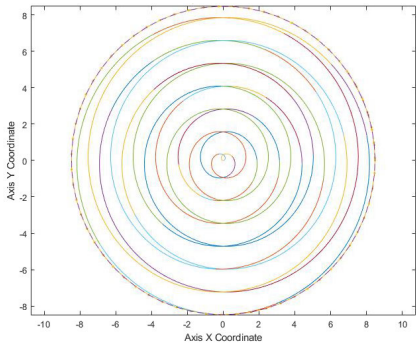

FIGURE 5. The synthetic trajectory of SLMM.

The node selects some parameters of mobility before movement, which includes the angular speed, the ending time and the time interval of moving and pausing. Then, the node follows the trajectory of spiral line of spreading outwardly until the moving time interval elapses, after that it hovers over the current location during the pausing time interval. Once approaches the boundary, the node immediately switches from the current trajectory to the new trajectory which will follow the spiral line of contracting inwardly.

Similarly, the node will spread outwardly again when it approaches the center of trajectory of spiral line. Finally, the node will repeat the entire process until the ending time has been finished.

B. THE VALIDATION OF SYNTHETIC TRAJECTORY OF SLMM

In order to validate synthetic trajectory, we should introduce some realistic mobility features extracted from real traces into the SLMM.

Firstly, we deploy a DJI Phantom 3 SE UAV in the playground and collect the real traces with the WGS84 coordinate. Next, we process the real data of traces, which includes the coordinate transformation and the reduction of noise, and obtain the optimal traces of aerial node (see Figure 6). Then, we extract and evaluate some information of mobility form the real traces, such as speed and moving time interval. Finally, we introduce these realistic mobility features into the SLMM, thereby produce the traces-based trajectory of SLMM (see Figure 7).

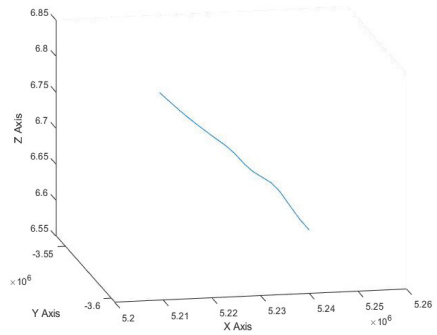

FIGURE 6. The real traces of aerial node.

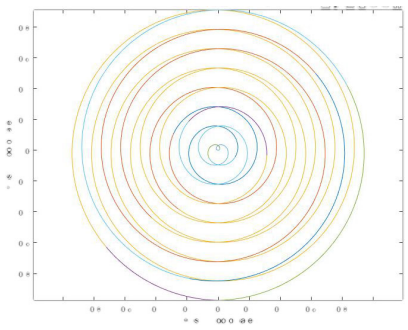

FIGURE 7. The traces-based trajectory of SLMM.

Obviously, the traces-based trajectory of SLMM is almost similar with the synthetic (see Figure 5,7). Therefore, it is validated through the real traces that the synthetic trajectory of SLMM is credible and authentic.

C. THE NOVEL BOUNDARY MODEL IN SLMM

Considered the aviation safety, the aerial node needs a buffer around the minimum safe zone, thereby has enough time to avoid crash [26]. Moreover, the aerial node also requires a buffer of communication, because the previous connection will be severely influenced by other node [28]. As a result, the aerial node could not greatly cooperate with each other to complete the mission. Hence, the annular buffer should be considered when the aerial node approaches the boundary of zone.

Here, we introduce the concept of buffer into SLMM and extend it to circular zone, thereby propose a novel annular boundary model.

Compared with the rectangular the annular boundary model has more authenticity, such that it could accurately reflect the real situation of boundaries. Obviously, the novel boundary model could greatly limit the trajectory of SLMM to the annular buffer (see Figure 8). In the contrast, the aerial node could reach the boundary without the boundary model, so that maybe suffer the effect of boundary (see Figure 5).

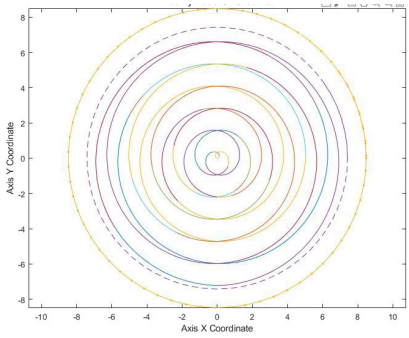

FIGURE 8. The trajectory of SLMM With novel boundary model.

D. THE CHARACTERISTICS AND ADVANTAGES OF SLMM

Intuitively, the SLMM has some inherent advantages and characteristics compared with RWP, ST and SRCM (see Figure 1, 3, 4).

Firstly, the prominent feature is the smooth trajectory other mobility model does not possess. It means that the SLMM has higher space-time correlation, such that it could simulate the mechanical and aerodynamic constraints in the aerial scene. Secondly, due to the mathematical feature the interval of trajectory of spiral line always is equal. It means that the aerial node could uniformly search the target zone under the SLMM. Thirdly, the trajectory of spiral line could gradually search the target zone without extra paths. It means that the aerial node could rapidly cover the target zone compared with other models. Finally, the aerial node possesses a search center and the capacity of hovering which is important for searching rapidly under the SLMM.

In short, compared with other mobility model the SLMM is more authentic for capturing accurately the aerial mobility in the SAR.

Next, we will investigate the mathematical feature of SLMM, includes the expression, the PDF and FDF of spatial node at steady state.

IV. THE ANALYTICAL FRAMEWORK OF MATHEMATICAL FEATURE OF SLMM

In this section, we will present an analytical framework to investigate some mathematical features of SLMM. Firstly, we deduce the specific expression of SLMM. Then, we estimate the PDF and FDF of spatial node at steady state under the SLMM. Finally, we validate the theoretical result through simulation.

A. THE EXPRESSION OF SLMM

According to the mechanism of SLMM, we could extract the mathematical process. Certainly, we still obey the previous assumption of mobility in the SLMM. Here, some special symbols are given to represent the mobility parameter (see the Table 1).

TABLE 1. The symbols of mobility parameter.

Symbol	Quantity
T_{End}	ending time
$T_{Current}$	current time
T_{Later}	later time
$\varphi_{Current}$	current radian
φ_{Later}	later radian
B_{Spiral}	thread pitch of spiral line
W_{move}	angular speed
T_{move}	moving time interval
T_{pause}	pausing time interval
(X,Y)	node coordinate
$\varphi_{\max}$	maximum polar angle
T_{Cycle}	time of a cycle
$F(\varphi)$	frequency density function (FDF)
$C(\varphi)$	cumulative distribution function (CDF)
$P(\varphi)$	probability density function (PDF)

Firstly, the aerial node selects some parameters before movement, includes $W_{move}, T_{move}, T_{pause}$. Then, the node moves with these parameters until the T_{move} elapses, after that the node hovers over current location during the T_{pause}.

Here, we extract above process with mathematical formulas.

$$\begin{aligned} \Delta\varphi &= W_{move} \times T_{move} \\ T_{Later} &= T_{Current} + T_{move} + T_{pause} \end{aligned} \tag{1}$$

Notes that φ_{Later} and T_{Later} mean that the corresponding radian and running time when the node reaches current destination.

Then, if the node follows the trajectory of spiral line of spreading outwardly, the process will satisfy under formulas.

$$\begin{aligned} \varphi_{Later} &= \varphi_{Current} + \Delta\varphi \\ D_{Start} &= \sqrt{X_{Start}^2 + Y_{Start}^2} \\ I_{Spiral} &= D_{Start} + B_{Spiral} \times \varphi \\ X &= I_{Spiral} \times \cos(\varphi) \\ Y &= I_{Spiral} \times \sin(\varphi) \end{aligned} \tag{2}$$

Notes that the current trajectory of node could be produced by above formulas in which φ switch from $\varphi_{Current}$ to φ_{Later}.

Similarly, if the node follows the trajectory of spiral line of contracting inwardly, the process will obey under formulas.

$$\begin{aligned} \varphi_{Later} &= \varphi_{Current} - \Delta\varphi \\ D_{Start} &= \sqrt{X_{Start}^2 + Y_{Start}^2} \\ I_{Spiral} &= D_{Start} + B_{Spiral} \times (-\varphi) \\ X &= I_{Spiral} \times \cos(-\varphi) \\ Y &= I_{Spiral} \times \sin(-\varphi) \end{aligned} \tag{3}$$

Finally, the node repeat entire process until the current time goes beyond the ending time (i.e. $T_{Current} > T_{End}$).

Clearly, compared with other mobility model the SLMM has the specific expression whatever spreading outwardly and contracting inwardly, which is important for statistical analysis of mobility model.

B. THE PDF OF SPATIAL NODE IN SLMM

For the sake of clarity, we present the theorem of PDF at first and then give its process of proof.

Theorem 1: We assume that the maximum polar angle of aerial node is $\varphi_{\max}$ and the thread pitch of spiral line is B_{Spiral}. Then, the PDF of spatial node is the uniform distribution at steady state under the SLMM and could be expressed as below.

$$P(\varphi) = \frac{1}{B_{Spiral}} \left[\varphi_{\max} \sqrt{\varphi_{\max}^2 + 1} + \ln\left(\varphi_{\max} \sqrt{\varphi_{\max}^2 + 1} \right) \right] \tag{4}$$

Notes that the details of proof are given in Appendix A.

For the aerial backbone networks, the spatial node of uniform distribution could permit a series of relevant results of network performance [15]. For example, we could directly abstract the graph of connectivity under the SLMM with the random geometry graph model (RGG) [28]. Therefore, some relevant results (e.g. connectivity [28]–[30], capacity [28], [31] and routing [32]) could help analyze the network performance under the SLMM.

C. THE FDF OF SPATIAL NODE IN SLMM

Similarly, we propose the theorem of FDF at first, and then its proof will be provided.

Theorem 2: We assume that the ending time of aerial node is sufficient under the SLMM. Thus, the limitation of $F(\varphi)$ could be expressed as below.

$$\lim_{t \to \infty} F(\varphi) = \frac{\varphi}{B_{Spiral}} \left[\varphi_{\max} \sqrt{\varphi_{\max}^2 + 1} + \ln\left(\varphi_{\max} \sqrt{\varphi_{\max}^2 + 1} \right) \right] \tag{5}$$

Notes that the details of proof are given in Appendix B.

Certainly, the FDF of spatial node is another important perspective for the mathematical features of mobility model. Compared with the PDF the FDF intuitively reflects the situation of distribution of spatial nodes within the entire zone.

In addition, the limitation of FDF will approximate with the value of CDF if the ending time is sufficient. Hence, we could accurately analyze the distribution of spatial nodes of mobility model with FDF. In short, it is inspiring that finding the role of FDF for the mobility model, and we will continue to study it in the future.

D. THE VALIDATION OF STATISTICAL RESULTS

Firstly, we configure some necessary parameters in the simulation. For the sake of data volume, we choose same ending time and the size of zone in the different model. Here, the ending time is 3000s and the size of the zone is 15m. In addition, we select appropriate parameters to guarantee that the mobility of each step is as consistent as possible under different mobility model. Here, the maximum running speed of aerial node is 10m/s and the maximum angular speed is pi/2 rad/s. Besides, the mean and variance of time interval of moving and pausing are all selected as 10 and 1, respectively.

Then, we implement the simulation at Matlab2019, and obtain the experimental results.

Clearly, the spatial nodes show the situation of different distribution under different mobility model.

Firstly, it is validated that the PDF of spatial nodes is the uniform distribution under the SLMM (i.e. Theorem 1) (see Figure 13). Similarly, the PDF of spatial nodes also is the uniform distribution under the SRCM (see Figure 12). On the contrary, most nodes irregularly distribute within central zone under the RWP (see Figure 9). This is because the node could randomly select the destination within entire zone. According to the central-limit theorem, the destination will be selected within central zone with high probability (i.e. the density wave [10]). Unexpectedly, the spatial nodes do not show the uniform distribution under the ST (see Figure 10), and at least it is not in theory [9]. The possible reason is that the existence of change of sharp direction or the lack of data volume. Besides, most nodes approximately distribute the central line of the zone under the BGMM (see Figure 11), because the selection of speed and direction based on the Markov-Chain, thereby a certain degree of correlation could be ensured between adjacent destination.

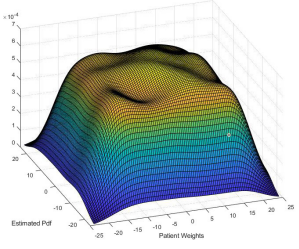

FIGURE 9. The PDF of RWP.

In the aspects of FDF, the spatial nodes also obviously show the different situation under different mobility model.

For example, the spatial node shows the FDF of irregular distribution under the RWP whatever with low precision and high precision (see Figure 14). The probable reason is the

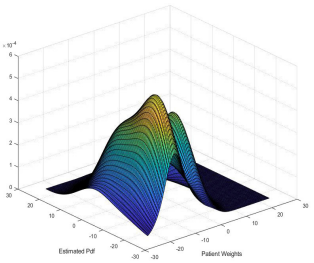

FIGURE 10. The PDF of ST.

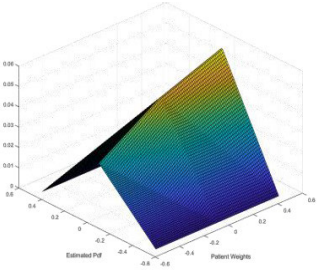

FIGURE 11. The PDF of BGMM.

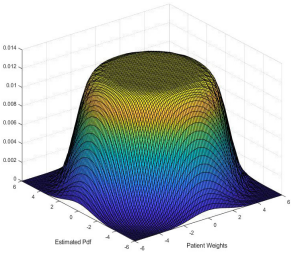

FIGURE 12. The PDF of SRCM.

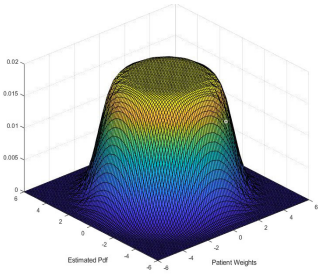

FIGURE 13. The PDF of SLMM.

randomness of adjacent destination of node (see Figure 1). In addition, the spatial node also shows the FDF of anomalous distribution under the ST (see Figure 15). The possible cause is the lack of data volume or some inherent defects (e.g. the absence of searching center or the instability of smooth trajectory) (see Figure 3). Besides, the spatial node of BGMM also shows the FDF of irregular distribution caused by the randomness of selection of speed and direction (see Figure 16).

On the contrary, the spatial node shows the FDF of almost uniform distribution under the SRCM and SLMM.

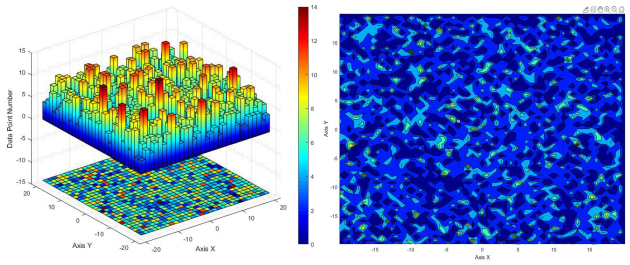

FIGURE 14. The FDF of RWP with low and high precision.

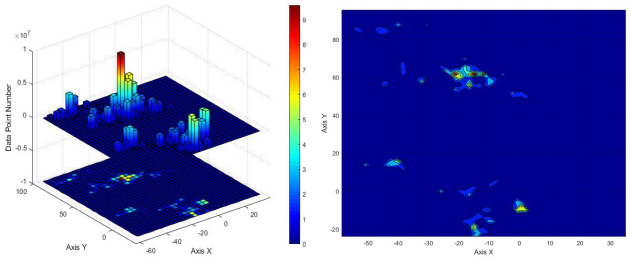

FIGURE 15. The FDF of ST with low and high precision.

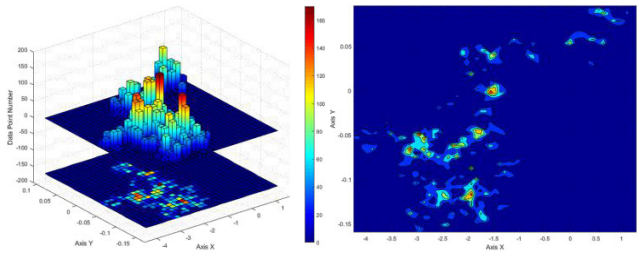

FIGURE 16. The FDF of BGMM with low and high precision.

Compared with SLMM, the FDF of spatial node appears a little nonuniform zone under the SRCM (see Figure 17). Partly, it is because the lack of data volume caused by the limited time. Nevertheless, the foremost reason is the randomness of selecting the radius of adjacent trajectory under the SRCM, thereby the distribution of switching paths of nodes is irregular (see Figure 4). In the contrast, the FDF of spatial node is like a series of concentric circles and uniformly distribute within the central zone under the SLMM (see Figure 18). That is because the distance between any adjacent trajectory is same and regular (see Figure 5). Therefore, the Theorem 2 has been validated.

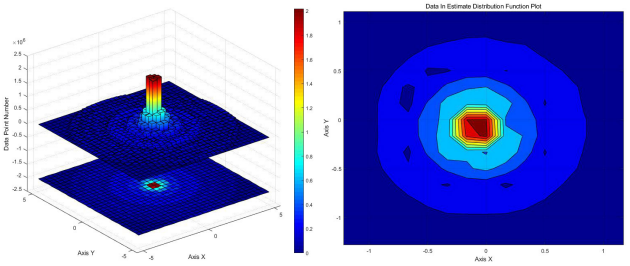

FIGURE 17. The FDF of SRCM with low and high precision.

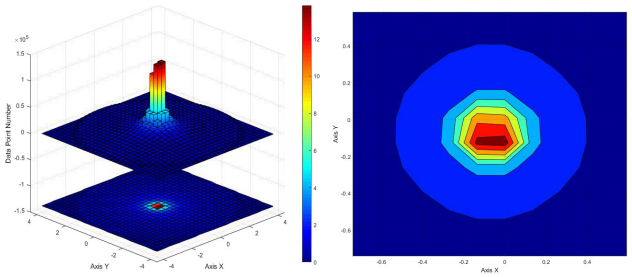

FIGURE 18. The FDF of SLMM with low and high precision.

Importantly, although the PDF of SRCM and SLMM are the uniform distribution, their FDF obviously appears some different features under high precision. Hence, it is very necessary that we deeply analyze the mathematical features of mobility model in the perspective of FDF.

Next, we will investigate some mobility features under the SLMM.

V. THE ANALYTICAL FRAMEWORK OF MOBILITY FEATURES OF SLMM

In this section, we will systematically study some mobility features of SLMM. Firstly, we discuss some necessary mobility features of AMM. Then, we propose and define some novel metrics to quantitatively analyze them (e.g. smoothness, coverage, randomness and boundary).

A. THE NECESSARY MOBILITY FEATURES FOR SAR

As mentioned before, the aerial node should follow some specific features of SAR under the AMM, especially mobility features.

Firstly, the foremost feature for AMM is the smooth trajectory. It means that the aerial node could accurately capture the space-time correlation caused by the mechanical and aerodynamic constraint.

In addition, an important feature is the coverage efficiency (e.g. the coverage ratio and the convergence time). Intuitively, that high coverage ratio means that the aerial node could search and cover more areas. Nevertheless, the aerial node should take more time in order to reach high coverage ratio. Thus, the convergence time must be considered because of the limitation of time. In short, the coverage efficiency should ensure the balance between the reliability and the availability.

Moreover, the randomness has been focused in other AMM (e.g. [9]) to estimate the degree of uncertainty of aerial trajectories. In the SAR, the aerial node should search and locate the ground victim as faster as possible, such that it does not take time to produce unnecessary paths. Hence, the randomness should be considered to obtain the optimal property of AMM.

As an ubiquitous problem, the boundary effect could directly affect aerial movement, thereby severely influence the network performance under the AMM [7], [9], [10]. Thus, the boundary effect is an inevitable issue for AMM.

B. THE DEFINITION OF MOBILITY METRICS

Firstly, we propose a novel metric called the degrees of smoothness to quantitatively analyze the smoothness of trajectory. For the sake of clarity, we give its definition at first.

Definition 1: We assume that the trajectory of node can be written as below forms of parametric equations.

$$\begin{aligned} X &= f(t) \\ Y &= g(t) \end{aligned} \tag{6}$$

Then, the curvature of trajectory can be expressed.

$$K(t) = \frac{\left| f'(t) g''(t) - f''(t) g'(t) \right|}{\left[f'^2(t) + g'^2(t) \right]^{3/2}} \tag{7}$$

Hence, we define the degrees of smoothness marked as SM(t) as below.

$$SM(t) = K'(t) \tag{8}$$

Specially, we will think this trajectory is smooth if the condition is true.

$$\lim_{t \to \infty} SM(t) > 0, \lim_{t \to \infty} SM(t) < 0 \tag{9}$$

In fact, the issue of smoothness of the curve has been studied in the region of DSP (e.g. [33]–[35]). Due to irregular variation of curvature, some unsmooth points of discontinuity maybe occur on curve [33]. In the contrast, the curvature of curve could monotonously change on the smooth trajectory. Here, we define the gradient of curvature as SM(t) (see Definition 1). Specially, we think this trajectory is smooth when the SM(t) is always positive or negative (i.e. the curvature monotonously change).

Next, we evaluate the coverage efficiency of AMM in two aspects, such as the coverage ratio and the convergence time. Similarly, we directly give the definition as below.

Definition 2: We assume that the entire area of the bounded zone could be represented as S and the searched zone could be marked as P(t). Then, we define the coverage ratio (CR) as below.

$$CR = \sup\left(\frac{P(t)}{S}\right) \tag{10}$$

In order to define another metric, we introduce a new symbol (i.e. $x = G[y(x)]$). It means that the corresponding value of independent variable x when the value of function equal with y(x).

Definition 3: Similarly, we define the convergence time (CT) as below.

$$CT = \inf G\left[\sup\left(\frac{P(t)}{S}\right)\right] \tag{11}$$

As mentioned above, the CR and CT both are focused to evaluate the coverage efficiency of AMM in different aspects. Clearly, the CR means that the maximum ratio of the searched zone in entire zone (see Definition 2). In addition, the CT means that the corresponding time when the AMM has reached maximum coverage (see Definition 3).

Besides, we estimate the randomness of AMM with the existing method (e.g. [9]). Here, we utilize the unique property of entropy to standardize the description that the entire randomness approximate with the sum of entropy of each parameter when each parameter is independent with each other. Then, we define the randomness (H_{all}) as below.

Definition 4: We assume that each model parameter, which the total quantity is N, all are independent with each other and the relative possibilities could be marked as P_i. According to the definition in [9], the entropy of each parameter could be expressed as below.

$$H_i = -\int P_i \ln P_i \tag{12}$$

Then, the H_{all} could be defined as below.

$$H_{all} = \sum_{i=1}^{N} H_i \tag{13}$$

Obviously, we define the as H_{all} the sum of entropy of each parameter (see Definition 4). In fact, the randomness is equivalent to the joint entropy for AMM.

In the further, we present a novel metric called the degree of boundary constraint (BC) to simulate the situation of boundaries of AMM. Here, we give its definition as below.

Definition 5: We assume that the entire area of the zone is defined as S. Besides, the connected range of devices is selected as R_{com}. Then, we define the BC as below.

$$BC = \inf \frac{S}{\pi R_{com}^2} \tag{14}$$

Clearly, the denominator of the equation is the coverage area of communication. Hence, the BC means that the minimum ratio of the whole zone to the coverage area of communication (see Definition 5).

Notes that the boundary effect will severely influence the network performance under the AMM, especially the routing property [4]. Hence, we roughly evaluate the degree of boundaries constraint of AMM, thereby could evaluate the boundary effect for aerial backbone network with this metric in the future.

Next, we will evaluate some mobility features of SLMM with above metrics through simulation or calculation.

VI. THE SIMULATION AND CALCULATION OF MOBILITY FEATURES OF SLMM

In this section, we will widely evaluate some mobility features of SLMM. Firstly, we should configure some useful parameters before simulation. Then, we evaluate the smoothness and the coverage efficiency under different AMM through simulation. In addition, we roughly estimate the randomness and the degree of boundaries constraint under them through calculation.

Here, we simulate the rescue situation in maritime SAR. In this scenario, many tourists in a crashed steamship have fallen into water. The UAV as the aerial node will search and

cover the potential zone within 10m around the steamship and locate the location of each victim.

For the sake of convenience we select the different shape of searching zone under different mobility models, (i.e. the square zone in the RWP, BGMM, ST and the circular zone in the SRCM and SLMM). In order to ensure same search area, the searching radius of square zone is greater a little than the circular zone. Here, we select 7m and 4m in the square and circular zone, respectively.

Similarly, we select appropriate parameters to guarantee that the mobility of each step is as consistent as possible under different mobility model. For example, we select 10 m/s as maximum running speed of aerial node in the RWP, and pi/2 rad/s as maximum angular speed in the ST, BGMM, SRCM and SLMM, respectively. Moreover, the origin of coordinates is selected as the initial location of aerial node in each mobility model.

Then, we perform the simulation at Matlab2019, and investigate the mobility features of SLMM in the different aspects.

A. THE SIMULATION OF DEGREE OF SMOOTHNESS OF SLMM

For the sake of clarity, we run the simulation at least 20 times under each mobility model. In addition, we adopt the method of numerical approximation to reckon the differential coefficient in equation (7) and (8). Meanwhile, we optimize the current result through multiplying by the certain coefficient to ensure the credibility of approximate values. Moreover, we sum the current result with the appropriate precision to largely reduce data volume, which is inspired by the thought of calculus and partition. Finally, we obtain the optimal result as below.

Interestingly, the SM(t) always approximate with zero under the RWP (see Figure 19), but it does not mean its trajectory is smooth, because the path between any adjacent waypoint is the straight line which the curvature always is zero. Similarly, the SM(t) always is almost zero under the BGMM (see Figure 20), because the path of subsection of adjacent destination is constituted by the straight line which the curvature is zero.

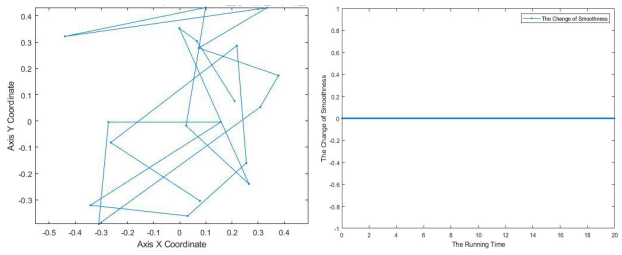

FIGURE 19. The trajectory of RWP and its degree of smoothness.

On the contrary, the SM(t) is not monotonous and occurs 5 and 11 trip points under SRCM and ST, respectively (see Figure 21, 22). It implies that the trajectory respectively has 5 and 11 unsmooth points in which the node maybe occurs the change of sharp direction. As mentioned before, the possible cause is switching randomly adjacent trajectory under the SRCM and switching unusually at adjacent interval under the ST, respectively. Hence, the trajectory of SRCM and ST all are not smooth.

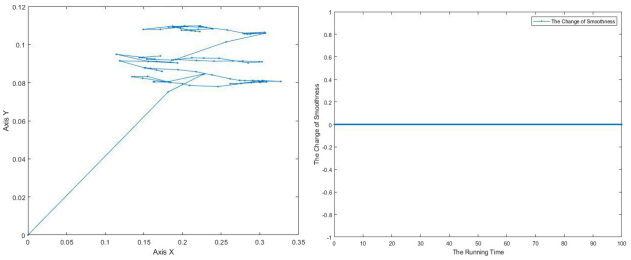

FIGURE 20. The trajectory of BGMM and its degree of smoothness.

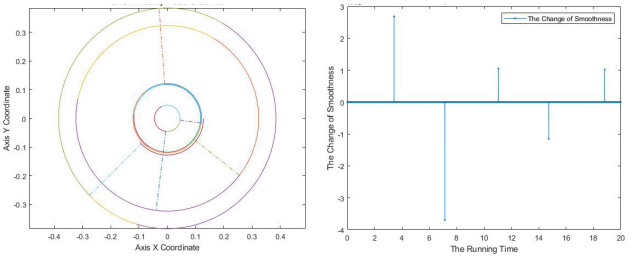

FIGURE 21. The trajectory of SRCM and its degree of smoothness.

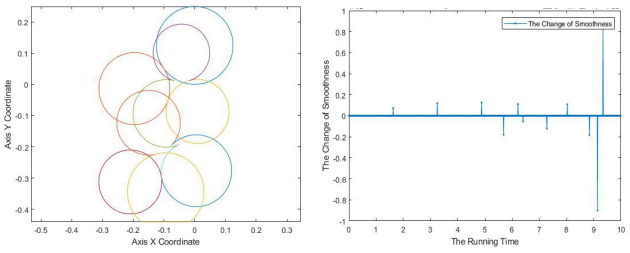

FIGURE 22. The trajectory of ST and its degree of smoothness.

Certainly, it is a smooth trajectory under the SLMM, because the SM(t) always approximate with zero (see Figure 23). That is because the node always follows the smooth trajectory of spiral line whatever spreading outwardly and contracting inwardly.

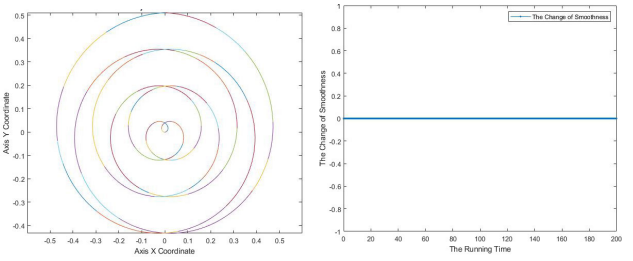

FIGURE 23. The trajectory of SLMM and its degree of smoothness.

In short, it is validated through simulation that the SM(t) is valid under different mobility model, and the trajectory of SLMM is only smooth compared with other mobility model.

B. THE SIMULATION OF COVERAGE EFFICIENCY OF SLMM

In order to reduce complexity, we sample the data of trajectories with low precision. Then, we reckon the area of searched zone under different mobility model, respectively. In the further, we could obtain both results of CR and CT. To improve credibility, we complete the simulation at least 100 times and calculate their confidence interval of 95%. Finally, we acquire optimal result of coverage efficiency as below.

At the aspect of CR, it is obvious that the ST merely has the CR of 18% (see Figure 24), that is because the node will randomly move within entire zone due to absence of search center, even could not turn back to zone after some cycles. Thus, the searched area is very limited. Similarly, the searched area also is few and the CR is almost 28% under the BGMM. The probable cause is the high correlation of adjacent destination, such that most nodes distribute mainly within the limited zone. Moreover, the SLMM just has the CR of 40% with the thread pitch of 0.02. That is because the distance of adjacent trajectory is larger, such that the searched area is little. Nevertheless, the CR will increase gradually with the thread pitch increase under the SLMM, because the distance of adjacent trajectory could decrease gradually with the thread pitch increase, thereby the searched area will increase. In addition, the CR could approach 100% under the SRCM, because the node finally covers the whole zone when its radius traverses entire range.

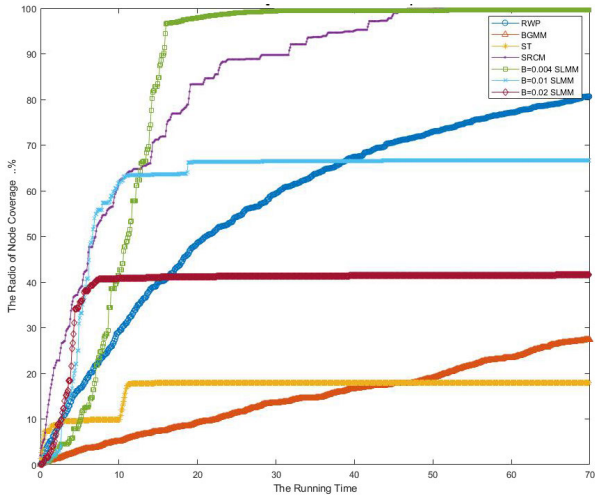

FIGURE 24. The coverage efficiency with 95% confidence Interval.

At the aspect of CT, the RWP has the CT of more than 70s (see Figure 24). It is because the node could randomly select the destination within entire zone, thereby will spend a lot of time on the overlapped path. Similarly, the CT is also over 70s under the BGMM because of the high correlation of adjacent destination, thereby the node must cost more time to cover whole zone. Besides, the ST has the CT of 12s, that is because the node could rapidly approach steady state with few searched area. In addition, the SRCM has the CT of 47s, that is because the node could randomly select the adjacent trajectory, such that the next trajectory maybe overlaps the previous. On the contrary, the SLMM has the CT of 8s with the thread pitch of 0.02, because the node could spread outwardly with faster speed, thereby could cover whole zone within few cycles. Meanwhile, the CT will increase gradually with the thread pitch decrease in SLMM. Specially, the CT is almost 27s with the 100% coverage under the SLMM. That is because the distance of adjacent trajectory will reduce gradually with the thread pitch decrease (i.e. the spreading speed of spiral line will decrease).

In short, the SLMM possesses shorter CT with the CR of 100% compared with other mobility model. Meanwhile, the CR and CT of SLMM could be adjusted through changing the thread pitch of spiral line to obtain optimal coverage efficiency. Certainly, it is an unique advantage for the capacity of aerial communication. Specially, the optimal coverage efficiency could be obtained when the thread pitch of spiral line approximate with a half of connected range of node.

C. THE CALCULATION OF RANDOMNESS OF SLMM

For the sake of space, we directly introduce some results of randomness under the ST and SRCM in [9].

$$H_{ST} = -(1-\lambda\Delta t)\ln(1-\lambda\Delta t) - \lambda\Delta t \ln\frac{\lambda\Delta t}{\sqrt{2\pi e\sigma}}$$
$$H_{SRCM} = -\frac{1}{r_o - r_i}\ln\frac{1}{r_o - r_i}\frac{V\Delta t}{2\pi}(\ln r_o - \ln r_i) \quad (15)$$

In addition, due to the speed of node do not affect the randomness of RD [9], thus the randomness of RWP and BGMM approximate with the RD.

$$H_{RWP,BGMM} = -(1-\lambda\Delta t)\ln(1-\lambda\Delta t) - \lambda\Delta t \ln\frac{\lambda\Delta t}{2\pi} \quad (16)$$

Notes that these details of calculation could be found in [9].

Next, we reckon the randomness of SLMM. Firstly, we assume that the angular speed w is the uniform distribution between the range $[0, W_{\max}]$. Besides, the time interval Δt is the exponential distribution with the coefficient λ in SLMM.

$$f_w = \frac{1}{W_{\max}} (0 < w < W_{\max})$$
$$f_{\Delta t} = \lambda e^{-\lambda t} (t > 0) \quad (17)$$

Then, we investigate the possibility at each time Δt considering the similar analysis in [9]. As Δt is sufficiently small, we assume that the change of direction appears at most once within Δt [9]. In addition, the possibility of changing the direction K times within Δt is marked as $P(n = k)$. Hence, we could know that $P(n = 1) = 1$, because the direction of node always changes in SLMM. Certainly, the change of angle of node and the relative probability can be obtained

as below.

$$\varphi = w\Delta t$$
$$f_{\varphi}(t) = \frac{\lambda}{W_{\max}} e^{-\lambda t} \ (t > 0) \tag{18}$$

In the further, we could calculate the H_{all} of SLMM as below.

$$\begin{aligned} H_{SLMM} &= -\int_0^{\infty} \frac{\lambda}{W_{\max}} e^{-\lambda t} \ln \frac{\lambda}{W_{\max}} e^{-\lambda t} dt \\ &\xrightarrow{x = \frac{\lambda}{W_{\max}} e^{-\lambda t}} \int_0^{\frac{\lambda}{W_{\max}}} x \ln x \cdot (-\frac{W_{\max}^2}{\lambda^2} \frac{1}{x}) dx \\ &= -\frac{W_{\max}^2}{\lambda^2} \int_0^{\frac{\lambda}{W_{\max}}} \ln x dx \\ &= -\frac{W_{\max}^2}{\lambda^2} (x \ln x - x|_0^{\frac{\lambda}{W_{\max}}}) \\ &= -\frac{W_{\max}}{\lambda} (\ln \frac{\lambda}{W_{\max}} - 1) \end{aligned} \tag{19}$$

As a result, the angular speed positively affects the H_{all} of SLMM. And the H_{all} will decrease gradually with the λ increase (see Equation (19)). The result is reasonable, because the increase of angular speed means that the change of direction will improve, thereby increase a certain degree of randomness. Similarly, increasing the λ means that the time interval will change more frequently, and the change of direction will reduce, thereby decrease a certain degree of randomness. In short, the H_{all} of SLMM is relatively few compared with other mobility model.

D. THE CALCULATION OF DEGREE OF BOUNDARY CONSTRAINT OF SLMM

Considering the convenience, we assume that the searched zone is square which the size of side is b in each mobility model (i.e. $S = b^2$). In addition, the aerial space is almost only two paths and the connected range is 0.2 km (i.e. $R_{com} = 0.2km$).

Here, we roughly evaluate the range of BC according to the application scenario under different mobility model.

First of all, the RWP is very common in the different application (e.g. the coverage, cruise, search, aerial transport). Similarly, the BGMM is also usual to simulate the movement of body node (e.g. human, animal). Hence, the length of boundaries is different in the different application. For example, the length of boundaries is less than 1km in cruise. In the contrast, the length of boundaries is more than 10000km in aerial flight. Then, we roughly evaluate the range of BC under the RWP and BGMM as below.

$$BC_{RWP,BGMM\_low} = \frac{b_{low}^2}{\pi R_{com}^2} \approx \frac{1^2}{\pi \times 0.2^2} = 7.96$$
$$BC_{RWP,BGMM\_high} = \frac{b_{high}^2}{\pi R_{com}^2} \approx \frac{10000^2}{\pi \times 0.2^2} = 7.96 \times 10^8$$
$$\therefore BC_{RWP,BGMM} \subset \left[7.96, 7.96 \times 10^8\right] \tag{20}$$

However, the ST, SRCM and SLMM aim to a specific application, thereby their range of BC is relatively narrow. For example, the length of boundaries of investigation approximate with order of 10km and 100km under the ST. Hence, we calculate the range of BC under the ST as below.

$$BC_{ST\_low} = \frac{b_{low}^2}{\pi R_{com}^2} \approx \frac{10^2}{\pi \times 0.2^2} = 7.96 \times 10^2$$
$$BC_{ST\_high} = \frac{b_{high}^2}{\pi R_{com}^2} \approx \frac{100^2}{\pi \times 0.2^2} = 7.96 \times 10^4$$
$$\therefore BC_{ST} \subset \left[7.96 \times 10^2, 7.96 \times 10^4\right] \tag{21}$$

Similarly, the SRCM and SLMM mainly face with the application of search and rescue, thereby its length of boundaries approximate with order of 0.1km and 10km. Thus, we reckon their range of BC as below.

$$BC_{SR\_SL\_low} = \frac{b_{low}^2}{\pi R_{com}^2} \approx \frac{0.1^2}{\pi \times 0.2^2} = 7.96 \times 10^{-2}$$
$$BC_{SR\_SL\_high} = \frac{b_{high}^2}{\pi R_{com}^2} \approx \frac{10^2}{\pi \times 0.2^2} = 7.96 \times 10^2$$
$$\therefore BC_{SR\_SL} \subset \left[7.96 \times 10^{-2}, 7.96 \times 10^2\right] \tag{22}$$

Obviously, we find that the BC are relatively wide under the SRCM and SLMM, but the RWP is not. This consequence is credible, because the node must be limited within the target zone in search and rescue, so that its boundary constraint is very strict. On the contrary, the node should transfer from a location to the other which the adjacent distance is usually large, thereby its boundary constraint is relatively loose in aviation or aerial transportation. Hence, we can obtain the rough result of BC based on its range (See the TABLE 2).

TABLE 2. The Level of boundary constraint.

	RWP	BGMM	ST	SRCM	SLMM
BC	$[10^0,10^8]$	$[10^0,10^8]$	$[10^2,10^4]$	$[10^{-2},10^2]$	$[10^{-2},10^2]$
Constraint	Loosest	Loosest	Moderate	Strictest	Strictest

Next, we will investigate the network performance of aerial backbone network under the SLMM.

VII. THE NETWORK PERFORMANCE OF AERIAL BACKBONE NETWORK UNDER SLMM

In this section, we will evaluate network performance under the SLMM with the Table-Driven (e.g. DSDV [38], [39]) and the Link-Driven routing protocol (e.g. AODV [36], [37], DSR [40], [41]) which are usually utilized to evaluate the network. Firstly, we select appropriate parameters before simulation. Then, we briefly describe the whole procedure how to setup and perform this simulation. Finally, we evaluate the network performance under different AMM (e.g. throughput, end-end delays, packet loss rate and routing overhead).

Similarly, we still simulate the rescue situation in the maritime SAR. But here, we assume that the potential searching zone is the region around the steamship within 1000m.

In order to generate mobility files, the searching radius all is selected as 1000m, and the searching time all is configured as 200s in different mobility model. In addition, the number of nodes all is 20 and the connected range of each node all is 200m. Moreover, the initial location of each node is the center of whole searching zone. In addition, the maximum running speed and angular speed is configured as 10 m/s and pi/2 rad/s, respectively. Besides, the mean and variance of time interval of running and pausing all are selected as 10 and 1, respectively. Specially, the maximum radius all are configured as 500m under the SRCM and SLMM, and the thread pitch of spiral line is the 40% length of connected range.

With the above mobility files, we construct the aerial backbone networks in the NS2 simulator. Firstly, we select the connected node of 10 and the sending rate of 0.1Mb/s in the CBR generator to obtain the CBR stream file. In addition, we should configure some parameters of communication. For example, the propagation model and the MAC protocol are selected as the TwoRayground model and standard 802.11 protocol, respectively. Moreover, the transmitting frequency of nodes is 2GHz, and the receiving and transmitting antennas is Omniantenna with the power of 1W. Besides, the type of queues is DropTail with the maximum length of 1000. Then, we perform the simulation at the NS2 simulator, thereby obtain traces files which record entire situation of network during the simulation. In the further, we analyze traces files with AWK, and draw the experimental results on Gnuplot.

Here, we mainly evaluate the network performance under the DSDV and AODV protocol. Besides, the DSR protocol as a supplement will be briefly discussed under the SLMM to find the optimal routing protocol.

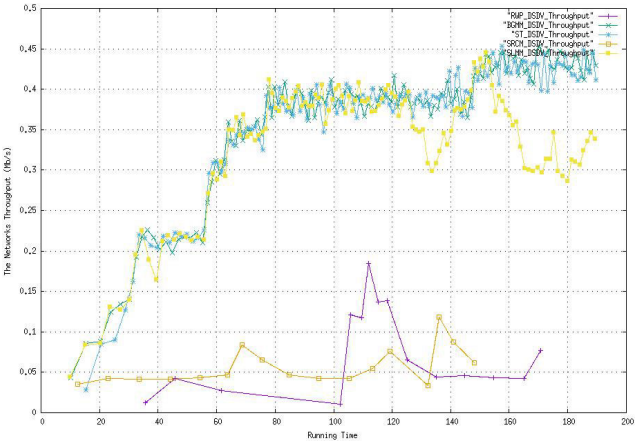

FIGURE 25. The network throughput of aerial networks (DSDV).

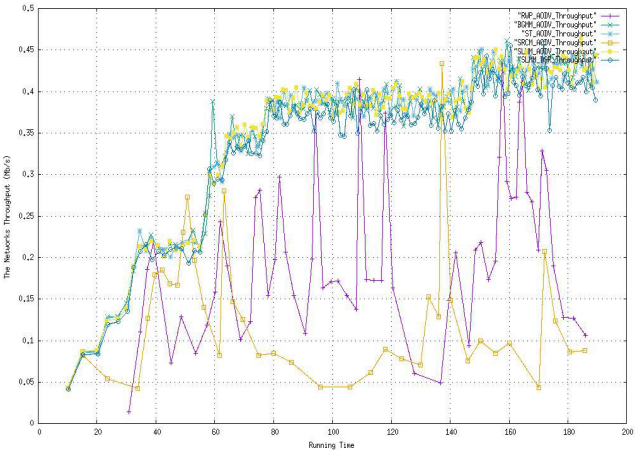

FIGURE 26. The network throughput of aerial networks (AODV, DSR).

A. THE NETWORK THROUGHPUT OF AERIAL BACKBONE NETWORK

With the DSDV protocol, the network throughput is relatively higher, and approximate with 0.42Mb/s, 0.40Mb/s and 0.38Mb/s under ST, BGMM and SLMM, respectively (see Figure 25). That is because the DSDV is a table-driven protocol, and its routing table will slightly change if the adjacent position of nodes is within the range of previous connection, thereby the network throughput could keep higher. Commonly, the node could maintain continuous moving under the ST, BGMM and SLMM, such that the adjacent location of nodes is relatively close and network throughput could keep higher. Nevertheless, the nodes maybe exceed the range of previous connection under the SLMM, such that the old routing table has outdated, and the throughput will decline. On the contrary, the network throughput is relatively lower all the time, and approximate with 0.05Mb/s and 0.06Mb/s under the RWP and SRCM, respectively. The possible cause is the randomness of selecting adjacent destination or trajectory under the RWP and SRCM, thereby the adjacent location of nodes will drastically change, and the network throughput could not keep high.

Obviously, we could find some similar results with the AODV protocol (see Figure 26). For example, the network could keep higher network throughput, and approximate with 0.42Mb/s, 0.41Mb/s and 0.43Mb/s under the ST, BGMM and SLMM, respectively. Besides, the network throughput is relatively lower, and approximate with 0.22Mb/s and 0.13Mb/s under the RWP and SRCM, respectively. However, it still exists a little difference between them. The probable reason is the AODV is a link-driven protocol, thereby the network will adopt a relatively shorter path when a packet should be transmitted, and its routing table could be updated real time before transmission. Hence, the connected link could maintain relatively shorter, such that the network throughput will improve a little compared with table-driven protocol.

In addition, we evaluate the aerial backbone network under the SLMM with better DSR protocol. The network throughput, though, does not obviously improve, and still approximate with 0.43Mb/s. The possible cause is that any connected link already is a shorter path under the link-driven protocol, thereby the DSR algorithm could not bring any obvious benefit.

B. THE END-TO-END DELAY OF AERIAL BACKBONE NETWORK

With the DSDV protocol, the end-to-end delay will change between 0ms and 4000ms and between 0ms and 3200ms under the RWP and SRCM, respectively (see Figure 27). That is because the DSDV is table-driven, thereby its routing table could stay fixed for a certain period. Hence, the connected link will be broken if the adjacent location of nodes exceed the connected range under the RWP and SRCM, thereby the end-to-end delay will rocket. In the contrast, the end-to-end delay could keep lower, and approximate with 5.5ms, 5.0ms and 4.8ms under the ST, BGMM and SLMM, respectively. It is because the adjacent location of nodes could not exceed the connected range, thereby the connected link could keep stable under the ST, BGMM and SLMM.

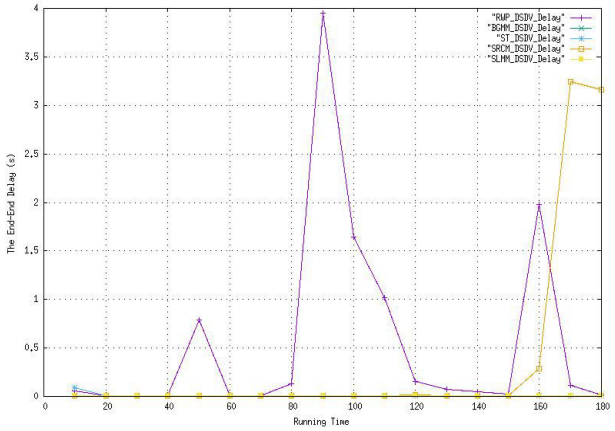

FIGURE 27. The end-end delay of aerial networks (DSDV).

However, we find some different results under the AODV protocol. For example, the end-to-end delay all will occur slight wobble except the SLMM (see Figure 28). In addition, the end-to-end delay is approximate with 800ms, 5.0ms, 5.2ms and 300ms under the RWP, ST, BGMM, SRCM, respectively. But, the SLMM could keep the end-to-end delay of 4.42ms all the time. The possible cause is the link-driven protocol could select the shortest path according to current location of node, thereby its routing table could be updated real time before each transmission. Hence, the connected link all could be automatically adjusted according to current location of nodes, thereby the end-to-end delay ultimately approaches stable.

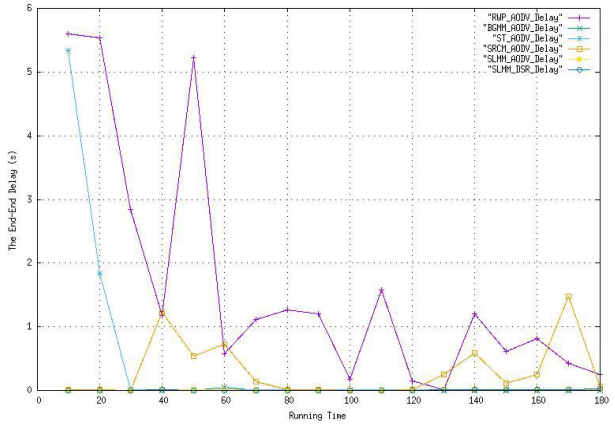

FIGURE 28. The end-end delay of aerial networks (AODV, DSR).

Specially, the network could keep the end-to-end delay of almost 4.45ms all the time whatever under the AODV and DSR protocol in the SLMM. The probable cause is that the adjacent location of nodes could not largely change under the SLMM, thereby any connected link already is the shortest path. Thus, the end-to-end delay could keep stable and lower all the time.

C. THE PACKET LOSS RATE OF AERIAL BACKBONE NETWORK

With the DSDV protocol, the packet loss rate keep higher all the time, and approximate with 85% and 83% under the RWP and SRCM, respectively (see Figure 29). That is because that the adjacent location of nodes maybe drastically changes, thereby the distances of them exceed the range of previous connections. Thus, the connected link will be broken with higher probability, such that more packets maybe are dropped in network. In the contrast, the network could keep lower packet loss rate all the time, and approximate with nearly 0.00%$_{\circ}$, 0.00%$_{\circ}$ and 0.01%$_{\circ}$ under the ST, BGMM and SLMM, respectively. The probable cause is the adjacent location of nodes only slightly changes, such that the connected link keeps the better situation. Hence, most packets could be reliably transmitted through network. In addition, the packet loss rate will go up a little at last under the SLMM. That is because adjacent distances of nodes will add as time go on, thereby maybe exceed the range of previous connections. Thus, the connected link already is not the shortest path, such that some packets will be dropped under the old routing table.

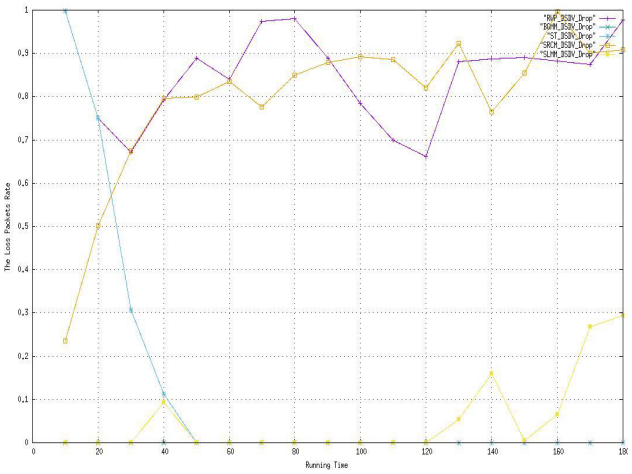

FIGURE 29. The packets loss rate of aerial network (DSDV).

Certainly, we can find some different results under the AODV protocol (see Figure 30). For example, the packet loss

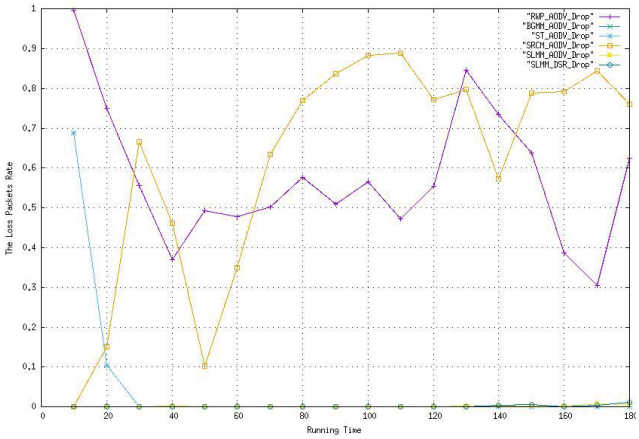

FIGURE 30. The packets loss rate of aerial network (AODV, DSR).

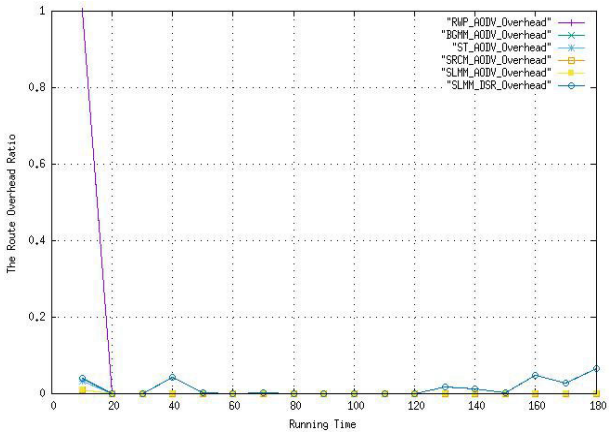

FIGURE 32. The route overhead of aerial network (AODV, DSR).

rate approximate with 55% and 70% under the RWP and SRCM, respectively. In the contrast, the packet loss rate is approximate with nearly 0.00%$_{\circ}$ under the ST, BGMM and SLMM. Their discrepancy is because the situation of connected link will largely improve if the routing table could be updated real time. Hence, most packets will not be dropped. With the AODV or DSR, the network could keep nearly 0.00%$_{\circ}$ packet loss rate all the time under the SLMM. That is because its routing table could also be updated real time.

D. THE ROUTING OVERHEAD OF AERIAL BACKBONE NETWORK

With the DSDV, the network always keeps the routing overhead of almost zero under each mobility model (see Figure 31). That is because the DSDV merely maintains local routing table without searching new path by routing packets. Similarly, the network could keep the routing overhead of almost zero under the AODV, but the beginning is not (see Figure 32). It is because the AODV must search the shortest path by routing packets before first transmission. Hence, the network exists a little routing overhead at beginning.

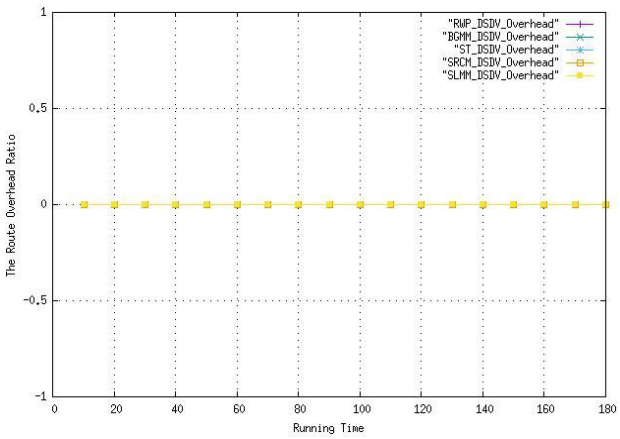

FIGURE 31. The route overhead of aerial network (DSDV).

Nevertheless, the AODV protocol will not search new path if the connected link could support local transmission, thereby the routing overhead will gradually go back to zero.

With the DSR, the routing overhead will occur a little slight wobble, and approximate with 3% under the SLMM. That is because the DSR devotes itself to search the shortest path by calculating the minimum time of all echoing packets. Therefore, some routing packets maybe appear before transmission.

In short, the aerial backbone network has higher throughput, lower end-to-end delay and lower packet loss rate under the SLMM. In addition, the better DSR could not provide some obvious benefits, in return maybe bring a little routing overhead under the SLMM. Therefore, the AODV is best routing choice for aerial backbone network under the SLMM.

VIII. CONCLUSION AND FUTURE WORKS

In this paper, we propose a novel AMM called as SLMM for aerial backbone network. Firstly, the SLMM has the specific expression, the PDF of uniform distribution and the FDF of symmetric distribution. Then, the SLMM possesses smooth trajectory all the time, thereby could accurately capture the space-time correlation in the aerial scene. In addition, the SLMM has superior coverage efficiency. Meanwhile, we could adjust some internal parameters to obtain optimal capacity of coverage. Besides, we evaluate the boundary constraint and the randomness of SLMM. In the further, we investigate the network performance under the SLMM. The result shows that the network has higher throughput, lower end-to-end delay and lower packet loss rate under the SLMM in which the AODV is best routing. In short, we believe that the SLMM as an important extension of AMM could help design a reliable and strong aerial backbone network.

In future work, we will extend the 2D SLMM to 3D, and evaluate mobility features and the network performance. Then, we will study the issue of connectivity for aerial backbone network under the 2D and 3D SLMM. Finally, we will investigate whether the dynamics of connectivity could affect the network performance under the SLMM.

APPENDIXES

APPENDIX A

Proof: To prove the theorem, a series of assumptions should be proposed before. Firstly, the time of each cycle is marked as T_{Cycle}. It means that the time of spreading outwardly or contracting inwardly approximate with a half of T_{Cycle} due to the symmetry relationship.

$$\varphi_{\max} = \sum_{t=0}^{\frac{T_{\text{Cycle}}}{2}} \Delta\varphi_t \tag{23}$$

Moreover, the thread pitch of spiral line has been selected before, and the initial location of each node is the origin of coordinates.

Next, we prove the theorem 1. According to definition, the PDF of SLMM could be expressed as below.

$$P(\varphi) = \frac{1}{L_{\text{Spiral}}} \tag{24}$$

Notes that L_{Spiral} represent the entire arc length of the trajectory of SLMM.

Then, we mainly calculate the L_{Spiral}. Firstly, we convert the expression of SLMM from rectangular coordinate form to polar form.

$$r(\varphi) = \sqrt{X^2 + Y^2} = D_{Start} + B_{\text{Spiral}} \times \varphi \tag{25}$$

Because the initial location of node is the origin of coordinate. That is

$$D_{Start} = \sqrt{X_{Start}^2 + Y_{Start}^2} = 0 \tag{26}$$

Thus, the expression of SLMM with polar form could be simplified as below.

$$r(\varphi) = B_{\text{Spiral}} \times \varphi \tag{27}$$

Then, we reckon the arc differential of the trajectory.

$$dl = \sqrt{r^2(\varphi) + r'^2(\varphi)}d\varphi = \sqrt{B_{\text{Spiral}}^2\varphi^2 + B_{\text{Spiral}}^2}d\varphi \tag{28}$$

Due to the symmetry relationship, the entire arc length of the trajectory of SLMM could be calculated as below.

$$\begin{aligned} L_{\text{Spiral}} &= \int_{-\infty}^{\infty} dl\,d\varphi = 2\int_0^{\varphi_{\max}} \sqrt{B_{\text{Spiral}}^2\varphi^2 + B_{\text{Spiral}}^2}d\varphi \\ &= 2B_{\text{Spiral}}\left[\frac{\varphi}{2}\sqrt{\varphi^2+1} + \frac{1}{2}\ln(\varphi + \sqrt{\varphi^2+1})\right]\Big|_0^{\varphi_{\max}} \\ &= B_{\text{Spiral}}\left[\varphi_{\max}\sqrt{\varphi_{\max}^2+1} + \ln(\varphi_{\max} + \sqrt{\varphi_{\max}^2+1})\right] \end{aligned} \tag{29}$$

Combined the equation (24) and (29), the PDF of SLMM could be found as below.

$$\begin{aligned} P(\varphi) &= \frac{1}{L_{\text{Spiral}}} \\ &= \frac{1}{B_{\text{Spiral}}\left[\varphi_{\max}\sqrt{\varphi_{\max}^2+1} + \ln(\varphi_{\max} + \sqrt{\varphi_{\max}^2+1})\right]} \\ &= \frac{1}{B_{\text{Spiral}}}\left[\varphi_{\max}\sqrt{\varphi_{\max}^2+1} + \ln(\varphi_{\max} + \sqrt{\varphi_{\max}^2+1})\right] \end{aligned} \tag{30}$$

At this point, the proof have been completed.

APPENDIX B

Proof: To prove the theorem, we assume the ending time of SLMM is sufficient. Next, we prove the theorem 2. Specially, the FDF will approximate with the CDF if the ending time is sufficient. And their relationship could be expressed as below.

$$\lim_{t\to\infty} C(\varphi) \approx F(\varphi) \tag{31}$$

According to the definition, the CDF of spatial node could be calculated as below under the SLMM.

$$\begin{aligned} &F(\varphi) \\ &= P\{\varphi' < \varphi\} \\ &= \int_{-\infty}^{\varphi} f_{\text{Spiral}}(\varphi')d\varphi' \\ &= \int_{-\infty}^{\varphi} \frac{1}{B_{\text{Spiral}}}\left[\varphi_{\max}\sqrt{\varphi_{\max}^2+1} + \ln(\varphi_{\max} + \sqrt{\varphi_{\max}^2+1})\right]d\varphi' \\ &= \frac{\varphi}{B_{\text{Spiral}}}\left[\varphi_{\max}\sqrt{\varphi_{\max}^2+1} + \ln(\varphi_{\max} + \sqrt{\varphi_{\max}^2+1})\right] \end{aligned} \tag{32}$$

Combined the equation (31) and (32), the limiting form of FDF of spatial node could be obtained at below under the SLMM.

$$\begin{aligned} &\lim_{t\to\infty} C(\varphi) \\ &\approx \lim_{t\to\infty} F(\varphi) \\ &= \frac{\varphi}{B_{\text{Spiral}}}\left[\varphi_{\max}\sqrt{\varphi_{\max}^2+1} + \ln(\varphi_{\max} + \sqrt{\varphi_{\max}^2+1})\right] \end{aligned} \tag{33}$$

At this point, the proof have been completed.

REFERENCES

[1] N. Aschenbruck and P. Martini, "Modeling public safety scenarios to evaluate wireless communication systems," in *Proc. 1st Int. Conf. Wireless Commun., Veh. Technol., Inf. Theory Aerosp. Electron. Syst. Technol.*, May 2009, pp. 510–514.

[2] S. Hayat, E. Yanmaz, and R. Muzaffar, "Survey on unmanned aerial vehicle networks for civil applications: A communications viewpoint," *IEEE Commun. Surveys Tuts.*, vol. 18, no. 4, pp. 2624–2661, 4th Quart., 2016.

[3] L. Gupta, R. Jain, and G. Vaszkun, "Survey of important issues in UAV communication networks," *IEEE Commun. Surveys Tuts.*, vol. 18, no. 2, pp. 1123–1152, 2nd Quart., 2016.

[4] J. Xie, Y. Wan, J. H. Kim, S. Fu, and K. Namuduri, "A survey and analysis of mobility models for airborne networks," *IEEE Commun. Surveys Tuts.*, vol. 16, no. 3, pp. 1221–1238, 3rd Quart., 2014.

[5] W.-J. Hsu, T. Spyropoulos, K. Psounis, and A. Helmy, "Modeling spatial and temporal dependencies of user mobility in wireless mobile networks," *IEEE/ACM Trans. Netw.*, vol. 17, no. 5, pp. 1564–1577, Oct. 2009.

[6] Z. Khan, P. Fan, and S. Fang, "On the connectivity of vehicular ad hoc network under various mobility scenarios," *IEEE Access*, vol. 5, pp. 22559–22565, 2017.

[7] A. Tiwari, A. Ganguli, A. Sampath, D. S. Anderson, B.-H. Shen, N. Krishnamurthi, J. Yadegar, M. Gerla, and D. Krzysiak, "Mobility aware routing for the airborne network backbone," in *Proc. IEEE Mil. Commun. Conf. (MILCOM)*, San Diego, CA, USA, Nov. 2008, pp. 1–7.

[8] J. P. Rohrer, E. K. Cetinkaya, H. Narra, D. Broyles, K. Peters, and J. P. Sterbenz, "AeroRP performance in highly-dynamic airborne networks using 3D Gauss-Markov mobility model," in *Proc. Mil. Commun. Conf. (MILCOM)*, Baltimore, MD, USA, Nov. 2011, pp. 834–841.

[9] Y. Wan, K. Namuduri, Y. Zhou, and S. Fu, "A smooth-turn mobility model for airborne networks," *IEEE Trans. Veh. Technol.*, vol. 62, no. 7, pp. 3359–3370, Sep. 2013.

[10] J. Harri, F. Filali, and C. Bonnet, "Mobility models for vehicular ad hoc networks: A survey and taxonomy," *IEEE Commun. Surveys Tuts.*, vol. 11, no. 4, pp. 19–41, 4th Quart., 2009.

[11] E. Kuiper and S. Nadjm-Tehrani, "Mobility models for UAV group reconnaissance applications," in *Proc. Int. Conf. Wireless Mobile Commun. (ICWMC)*, Bucharest, Romania, Jul. 2006, p. 33.

[12] S. Cabrero, X. G. Paneda, D. Melendi, R. Garcia, and T. Plagemann, "Using firefighter mobility traces to understand ad-hoc networks in wildfires," *IEEE Access*, vol. 6, pp. 1331–1341, 2018.

[13] M. Kim, D. Kotz, and S. Kim, "Extracting a mobility model from real user traces," in *Proc. 25th IEEE Int. Conf. Comput. Commun. (INFOCOM)*, 2006, pp. 1–13.

[14] J. Xie, Y. Wan, B. Wang, S. Fu, K. Lu, and J. H. Kim, "A comprehensive 3-dimensional random mobility modeling framework for airborne networks," *IEEE Access*, vol. 6, pp. 22849–22862, 2018.

[15] W. Wang, X. Guan, B. Wang, and Y. Wang, "A novel mobility model based on semi-random circular movement in mobile ad hoc networks," *Inf. Sci.*, vol. 180, no. 3, pp. 399–413, 2009.

[16] USA. (2018). *Drones May Aid Hurricane Relief Efforts*. [Online]. Available: https://uavcoach.com

[17] USA. (2019). *JTTUAV*. [Online]. Available: http://www.jttuav.com/article/detail/235.html

[18] USA. (2019). *Jay Manley*. [Online]. Available: https://courses.dronepro academy.com/courses

[19] Y. Zeng, R. Zhang, and T. J. Lim, "Wireless communications with unmanned aerial vehicles: Opportunities and challenges," *IEEE Commun. Mag.*, vol. 54, no. 5, pp. 36–42, May 2016.

[20] L. Reynaud, T. Rasheed, and S. Kandeepan, "An integrated aerial telecommunications network that supports emergency traffic," in *Proc. 14th Int. Symp. Wireless Pers. Multimedia Commun. (WPMC)*, Brest, Belarus, 2011, pp. 1–5.

[21] E. Mahdipour, E. Aminian, M. Torabi, and M. Zare, "CBR performance evaluation over AODV and DSDV in RW mobility model," in *Proc. Int. Conf. Comput. Autom. Eng.*, Bangkok, Thailand, Mar. 2009, pp. 238–242.

[22] C. Wang, J. Liu, and J. Kuang, "Performance analysis on direct transmission scheme under RWP mobility model in DTMSNs," in *Proc. 7th Int. Conf. Wireless Commun., Netw. Mobile Comput.*, Wuhan, China, Sep. 2011, pp. 1–4.

[23] Y. Gang, "SAR image rapid co-registration based on RD model and coherence interpolation," in *Proc. IEEE Int. Conf. Spatial Data Mining Geograph. Knowl. Services*, Fuzhou, China, Jun. 2011, pp. 370–372.

[24] K. Amjad, "Performance analysis of DSR protocol under the influence of RPGM model in mobile ad-hoc networks," in *Proc. 31st Int. Conf. Distrib. Comput. Syst. Workshops*, Minneapolis, MN, USA, Jun. 2011, pp. 100–104.

[25] A. Pal, J. P. Singh, P. Dutta, P. Basu, and D. Basu, "A study on the effect of traffic patterns on routing protocols in ad-hoc network following RPGM mobility model," in *Proc. Int. Conf. Signal Process., Commun., Comput. Netw. Technol.*, Thuckalay, India, Jul. 2011, pp. 233–237.

[26] Y. Wang and Y. Zhao, "Fundamental issues in systematic design of airborne networks for aviation," in *Proc. IEEE Aerosp. Conf.*, Big Sky, MT, USA, Aug. 2006, p. 8.

[27] J. Xie, Y. Wan, K. Namuduri, S. Fu, G. L. Peterson, and J. F. Raquet, "Estimation and validation of the 3D smooth-turn mobility model for airborne networks," in *Proc. IEEE Mil. Commun. Conf. (MILCOM)*, San Diego, CA, USA, Nov. 2013, pp. 556–561.

[28] N. M. Freris, H. Kowshik, and P. R. Kumar, "Fundamentals of large sensor networks: Connectivity, capacity, clocks, and computation," *Proc. IEEE*, vol. 98, no. 11, pp. 1828–1846, Nov. 2010.

[29] B. Gupta and A. Gupta, "On the k-connectivity of ad-hoc wireless networks," in *Proc. IEEE 7th Int. Symp. Service-Oriented Syst. Eng.*, Redwood City, CA, USA, Mar. 2013, pp. 546–550.

[30] A. Misra, G. Teltia, and A. Chaturvedi, "On the connectivity of circularly distributed nodes in ad hoc wireless networks," *IEEE Commun. Lett.*, vol. 12, no. 10, pp. 717–719, Oct. 2008.

[31] S. Diggavi, M. Grossglauser, and D. Tse, "Even one-dimensional mobility increases the capacity of wireless networks," *IEEE Trans. Inf. Theory*, vol. 51, no. 11, pp. 3947–3954, Nov. 2005.

[32] E. Kuiper and S. Nadjm-Tehrani, "Geographical routing with location service in intermittently connected MANETs," *IEEE Trans. Veh. Technol.*, vol. 60, no. 2, pp. 592–604, Feb. 2011.

[33] S. Lan and Y. Wan, "A non-parametric method for curve smoothing," in *Proc. IEEE 4th Int. Conf. Comput. Commun. (ICCC)*, Chengdu, China, Dec. 2018, pp. 1997–2001.

[34] M. Wenyan, J. Yongjie, X. Gang, and Q. Xaolin, "Study of α energy spectrum smoothing and appraising smoothing goodness," in *Proc. 8th Int. Conf. Electron. Meas. Instrum.*, Xi'an, China, Aug. 2007, pp. 1-73–1-76.

[35] S. A. Dianat, B. Brewington, and L. K. Mestha, "A multidimensional smoothing algorithm with applications to digital color printer calibration," in *Proc. 16th IEEE Int. Conf. Image Process. (ICIP)*, Cairo, Egypt, Nov. 2009, pp. 2025–2028.

[36] M. Singh and J. Sharma, "Performance analysis of secure & efficient AODV (SE-AODV) with AODV routing protocol using NS_2," in *Proc. 3rd Int. Conf. Rel., Infocom Technol. Optim.*, Noida, India, Oct. 2014, pp. 1–6.

[37] S. Tajik, G. Farrokhi, and S. Zokaei, "Performance of modified AODV (waiting AODV) protocol in mobile ad-hoc networks," in *Proc. 2nd Int. Conf. Ubiquitous Future Netw. (ICUFN)*, Jeju, South Korea, Jun. 2010, pp. 160–164.

[38] M. M. Morshed, F. I. S. Ko, D. Lim, M. H. Rahman, M. R. R. Mazumder, and J. Ghosh, "Performance evaluation of DSDV and AODV routing protocols in mobile ad-hoc networks," in *Proc. 4th Int. Conf. New Trends Inf. Sci. Service Sci.*, Gyeongju-si, South Korea, 2010, pp. 399–403.

[39] K. U. R. Khan, R. U. Zaman, A. V. Reddy, K. A. Reddy, and T. S. Harsha, "An efficient DSDV routing protocol for wireless mobile ad hoc networks and its performance comparison," in *Proc. 2nd UKSIM Eur. Symp. Comput. Modeling Simulation*, Liverpool, U.K., Sep. 2008, pp. 506–511.

[40] L. Pan, "An improved the DSR routing protocol in mobile ad hoc networks," in *Proc. 6th IEEE Int. Conf. Softw. Eng. Service Sci. (ICSESS)*, Beijing, China, Sep. 2015, pp. 591–594.

[41] Istikmal, "Analysis and evaluation optimization dynamic source routing (DSR) protocol in Mobile Adhoc network based on ant algorithm," in *Proc. Int. Conf. Inf. Commun. Technol. (ICoICT)*, Bandung, Indonesia, Mar. 2013, pp. 400–404.

[42] Y. Liu, D. Liu, and G. Yue, "BGMM: A body gauss-Markov based mobility model for body area networks," *Tinshhua Sci. Technol.*, vol. 23, no. 3, pp. 277–287, Jun. 2018.

[43] P. J. Singh and R. De Silva, "Design and implementation of an experimental UAV network," in *Proc. Int. Conf. Inf. Commun. Technol. (ICOIACT)*, Yogyakarta, Indonesia, Mar. 2018, pp. 168–173.

[44] S.-C. Choi, I.-Y. Ahn, J.-H. Park, and J. Kim, "Towards real-time data delivery in oneM2M platform for UAV management system," in *Proc. Int. Conf. Electron., Inf., Commun. (ICEIC)*, Auckland, New Zealand, Jan. 2019, pp. 1–3.

[45] A. Hanyu, Y. Kawamoto, and N. Kato, "On improving flight energy efficiency in simultaneous transmission and reception of relay using UAVs," in *Proc. 15th Int. Wireless Commun. Mobile Comput. Conf. (IWCMC)*, Tangier, Morocco, Jun. 2019, pp. 967–972.

[46] M. Mozaffari, W. Saad, M. Bennis, Y.-H. Nam, and M. Debbah, "A Tutorial on UAVs for wireless networks: Applications, challenges, and open problems," *IEEE Commun. Surveys Tuts.*, vol. 21, no. 3, pp. 2334–2360, 3rd Quart., 2019.

[47] S. Ur Rahman, G.-H. Kim, Y.-Z. Cho, and A. Khan, "Positioning of UAVs for throughput maximization in software-defined disaster area UAV communication networks," *J. Commun. Netw.*, vol. 20, no. 5, pp. 452–463, Oct. 2018.

DAWEI HE was born in Yanta, Xi'an, Shaanxi, China, in 1992. He received the B.S. degree in communication engineering from the Shaanxi University of Technology, Hanzhong, in 2010. He is currently pursuing the M.S. and Ph.D. degrees in aerospace science and technology with Xidian University, Shaanxi.

WEI SUN received the B.S. degree in measuring and control technology and the Ph.D. degree in circuit and system from Xidian University, Xi'an, China, in 2002 and 2009, respectively.

He is currently a Professor with the School of Aerospace Science and Technology, Xidian University. His current research interests include multi-UAV systems, visual information perception, pattern recognition, and embedded video systems.

LEI SHI received the B.S. degree in measurement and control and the Ph.D. degree in circuits and system from Xidian University, Xi'an, China, in 2006 and 2012, respectively.

From 2013 to 2014, he was a Lecturer with the School of Aerospace Science and Technology, Xidian University. Since 2015, he has been an Associate Professor with the TT&C and Communication Department, Xidian University. His research interests include aerospace TT&C and communications, EM propagation, and wireless channel modeling. In particular, a series of groundbreaking studies have been made on the channel modeling and communication methods for hypersonic/reentry vehicles communication.